

# Phase Locking via Brillouin-Enhanced Four-Wave-Mixing Phase Conjugation

Mark W. Bowers and Robert W. Boyd

**Abstract**—We show that it is possible to control with good accuracy the relative phase of several conjugate beams for a properly designed Brillouin-enhanced four-wave-mixing phase conjugation system. Three geometries, two that utilize two Brillouin cells and another that requires only one Brillouin cell, that achieve conjugate phase control are studied and many properties of each system are examined. We show that for our high-power laser application the one-cell geometry performs as well as or better than the other geometry. Phase control is shown to be useful for beam combination, vector phase conjugation, and optical path selection. A laser system that utilizes the one-cell geometry to enhance its performance is built and examined.

**Index Terms**—Birefringence, Brillouin scattering, optical phase conjugation, pulsed lasers, Q-switched lasers, YAG lasers.

## I. INTRODUCTION

IN THIS PAPER, the use of Brillouin-enhanced four-wave-mixing (BEFWM) optical phase conjugation is examined for phase locking multiple beams together and for its subsequent use in a phase-conjugate laser system. Phase locking of two or more beams under the appropriate conditions can be used for vector (polarization) phase conjugation [1]–[10], beam combination [11]–[18], and optical path selection [3], [4], [6]–[8]. Each of these applications of phase locking has been used to increase the output of a laser system or array beyond the power and beam quality possible without phase locking. The BEFWM process described in this paper is used to achieve vector phase conjugation, beam combination, and output path selection simultaneously. Several methods are shown, for the first time, to control the relative phases of the conjugate beams. Three geometries that can achieve this type of BEFWM and phase locking are examined and contrasted with each other. One of the BEFWM geometries is chosen to be used in a complete laser system.

Several methods for phase locking multiple beams have been previously examined, such as frequency-shifted and nonfrequency-shifted backward seeding [19], [20], single-seed stimulated Brillouin scattering (SBS) [13], [15]–[17],

[21], [22], BEFWM [4], [6]–[8], and four-wave-mixing in photorefractives [18]. Basov *et al.* [3] showed that in a conjugation process that introduces a frequency shift it is possible to adjust the relative phase between two beams by adjusting the relative optical path length. They found that the relative phase difference between the two beams can be determined by the equation

$$\Delta\phi = \Omega\Delta L/c \quad (1)$$

where  $\Delta L$  is the optical path length difference and  $\Omega$  is the frequency shift between the probe and the conjugate beams. Note that in a normal optical interferometer  $\Delta\phi = \omega\Delta L/c$  and for an ideal phase conjugate interferometer  $\Delta\phi = 0$ . Both vector phase conjugation and beam combination have been demonstrated [1]–[8], [11]–[17] under the condition  $\Delta\phi = 0$ .

Optical systems can have elements that introduce aberrations upon the optical wavefront and polarization. In order to fully correct for these aberrations it is necessary to create a beam that is not only a conjugate in the optical wavefront, as in conventional SBS, but also a conjugate of the polarization, unlike conventional SBS. A process that conjugates both the wavefront and the polarization is known as vector phase conjugation. Several methods have been used to correct for polarization distortions including vector phase conjugation [1]–[10] and polarization rotation compensation [23]–[25]. Conventional SBS, as mentioned above, does not conjugate the polarization and thus can be described as a scalar conjugation process [26]–[28]. In addition, conventional SBS has a random overall phase that can fluctuate randomly in a time of the order of five to six times the phonon lifetime [29]–[32]. It is possible to separate a beam into two orthogonal polarizations, conjugate each using scalar phase conjugation, and recombine them such that they emulate a vector phase conjugator, but only if the phases of each conjugate beam are locked together [1].

Vector phase conjugation has been successfully demonstrated using several different methods, such as; the Basov method of SBS [1]; BEFWM [3], [4], [6], [8]; saturable gain [9]; and saturable absorption [10]. While all of these methods are very good, they may not be suited for all applications. Only the methods presented in this paper and in [8] allow for multiple beams to be conjugated in separate regions of a BEFWM cell to reduce the thermal loading and relax the constraints of alignment. In addition, the methods presented in this paper allow for additional control over the characteristics of the conjugate beam through the polarization state of the pump beam.

Manuscript received March 27, 1997; revised December 22, 1997. This work was supported by the U.S. Department of Energy under Contract W-7405-Eng-48. The portion of this work performed at the University of Rochester was supported by the National Science Foundation Graduate Research Training under Grant GER-9553609 and the sponsors of the Center for Electronic Imaging Systems.

M. W. Bowers is with the Lawrence Livermore National Lab, Livermore, CA 94551 USA.

R. W. Boyd is with the Institute of Optics, University of Rochester, Rochester, NY 14627 USA.

Publisher Item Identifier S 0018-9197(98)02392-6.

Beam combining is usually achieved by splitting the probe beam into two or more spatially separated beams [1]–[7], [11]–[17]. Each of these probe beams is then conjugated and returns along its original path. If all of the phases of the probe beams are the same upon recombining then they will add in phase and recreate the original single input probe beam with good fidelity. This will occur if  $\Delta\phi = 0$  or  $2M\pi$ , where  $M$  is an integer. One advantage of beam combining in this manner is that the probe beam may be amplified in parallel small-diameter amplifiers to near their damage threshold. The beams are then recombined to make a single beam containing more energy than would be possible through any of the individual amplifiers without the possibility of optical damage.

Optical path selection, unlike beam combination, can utilize the value of  $\Delta\phi$  to select a unique optical path from several choices. For example, a value of  $\Delta\phi = 0$  may be used to select one path, while a value of  $\Delta\phi = \pi$  may select another. Optical path selection will be discussed further in Section III.

In this paper we will show that the phase difference,  $\Delta\phi$ , can be varied using any of several methods. We show what we believe to be the first experimental evidence that the polarization ellipticity of the pump can be used to control the relative phases of the probe beams. Each of these methods, such as the optical path length difference and the polarization ellipticity of the pump beam, can be used individually or all of the methods simultaneously for a more versatile system.

Three geometries of BEFWM were studied to determine which one had the best characteristics to achieve vector phase conjugation, beam combination, and optical path selection simultaneously. Two of the geometries utilized two Brillouin active cells and the third used just one cell. The complexity and potential benefits of each design is discussed.

Finally, a complete nearly diffraction-limited laser system is built using the one-cell geometry for BEFWM. The system characteristics and overall performance are discussed. It is shown that the system performance is significantly improved by the use of the BEFWM vector phase conjugation described in this paper.

## II. THEORY

In Fig. 1 we show a schematic of our BEFWM process. In this case, beams 1 and 2 are the pump and its conjugate, respectively, and beams 3 and 4 are the probe and its conjugate, respectively. It is important to note that in our system we use the normal definitions of pump and probe for a four-wave mixing process, but that unlike a normal four-wave mixing process our probe can be, and usually is, many orders of magnitude more intense than the pump. In order to describe the BEFWM process we start with the optical and acoustical wave equations [33] and make the slowly varying envelope approximation. We define the electric field vector as

$$\begin{aligned} \mathbf{E}_m(\mathbf{r}, t) &= \mathbf{A}_m(\mathbf{r}) \exp[i(\mathbf{k}_m \cdot \mathbf{r} - \omega_m t)] + \text{c.c.} \\ &= \{|A_{mx}(\mathbf{r})| \exp[i\phi_{mx}(\mathbf{r})] \hat{x} \\ &\quad + |A_{my}(\mathbf{r})| \exp[i\phi_{my}(\mathbf{r})] \hat{y}\} \\ &\quad \cdot \exp[i(\mathbf{k}_m \cdot \mathbf{r} - \omega_m t)] + \text{c.c.} \end{aligned} \quad (2)$$

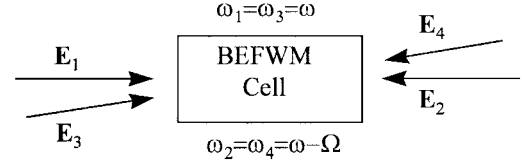


Fig. 1. A schematic of the BEFWM interaction showing the pump and probe relationships. The pump conjugate (beam 2) is shifted from the pump (beam 1) by the Brillouin frequency shift. The probe conjugate (beam 4) is also shifted by the same amount from the probe (beam 3).

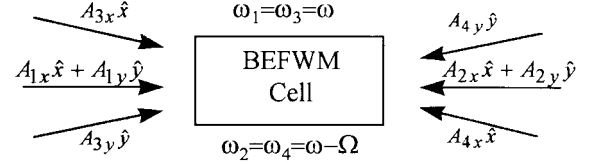


Fig. 2. The schematic of our system showing the physical separation of the probe and its conjugates into their polarization components.

From this definition of the slowly varying amplitudes we derive the following set of four coupled differential equations:

$$\frac{d\mathbf{A}_1}{dz} = \frac{-gc}{4\pi} [(\mathbf{A}_1 \cdot \mathbf{A}_2^*)\mathbf{A}_2 + (\mathbf{A}_1 \cdot \mathbf{A}_4^*)\mathbf{A}_4 \gamma^* + (\mathbf{A}_2^* \cdot \mathbf{A}_3)\mathbf{A}_4 \exp(-i\Delta\mathbf{k} \cdot \mathbf{r})\gamma^*] \quad (3a)$$

$$\frac{d\mathbf{A}_2}{dz} = \frac{-gc}{4\pi} [(\mathbf{A}_1^* \cdot \mathbf{A}_2)\mathbf{A}_2 + (\mathbf{A}_1^* \cdot \mathbf{A}_4)\mathbf{A}_3 \cdot \exp(-i\Delta\mathbf{k} \cdot \mathbf{r})\gamma + (\mathbf{A}_3^* \cdot \mathbf{A}_2)\mathbf{A}_3\gamma] \quad (3b)$$

$$\frac{d\mathbf{A}_3}{dz} = \frac{-gc}{4\pi} [\mathbf{A}_2(\mathbf{A}_1 \cdot \mathbf{A}_4^*)\gamma^* + (\mathbf{A}_2^* \cdot \mathbf{A}_3)\mathbf{A}_2 \cdot \exp(i\Delta\mathbf{k} \cdot \mathbf{r})\gamma^* + (\mathbf{A}_3 \cdot \mathbf{A}_4^*)\mathbf{A}_4], \quad (3c)$$

$$\frac{d\mathbf{A}_4}{dz} = \frac{-gc}{4\pi} [(\mathbf{A}_1^* \cdot \mathbf{A}_4)\mathbf{A}_1\gamma + \mathbf{A}_1(\mathbf{A}_2 \cdot \mathbf{A}_3^*) \cdot \exp(i\Delta\mathbf{k} \cdot \mathbf{r})\gamma + (\mathbf{A}_3^* \cdot \mathbf{A}_4)\mathbf{A}_3] \quad (3d)$$

where  $g$  is the Brillouin gain factor and  $\Delta\mathbf{k} \equiv \mathbf{k}_1 + \mathbf{k}_2 - \mathbf{k}_3 - \mathbf{k}_4$ . Only Brillouin resonant and nearly Brillouin resonant terms are included in this expression. The angular dependence of the Brillouin process is described by the factor

$$\gamma \equiv \frac{1}{1 + i\tau_B\Omega \sin^2 \frac{1}{2}\theta} \quad (4)$$

where  $\tau_B$  is the phonon lifetime and  $\theta$  is the angle between the pump and the probe.

In most of our work we have found it advantageous to split the probe beam  $\mathbf{A}_3$  into spatially separated  $x$  and  $y$  polarization components and treat each polarization component independently. A schematic of this geometry is shown in Fig. 2. If the probe beam  $\mathbf{A}_3$  is linearly polarized along either the  $x$  or  $y$  directions it becomes easy to calculate the phase of the conjugate beam  $\mathbf{A}_4$ . If the probe beam is  $x$  polarized then (3) reduces to a simplified version that we studied earlier [8]. The linearly polarized probe model was shown to predict the phase  $\mathbf{A}_{4x}$  to be given by

$$\phi_{4x} \cong \phi_{1x} + \phi_{2x} - \phi_{3x}. \quad (5)$$

A similar equation holds if the probe beam is  $y$  polarized. Numerical simulations of (3) show that even for 0.244 rad,

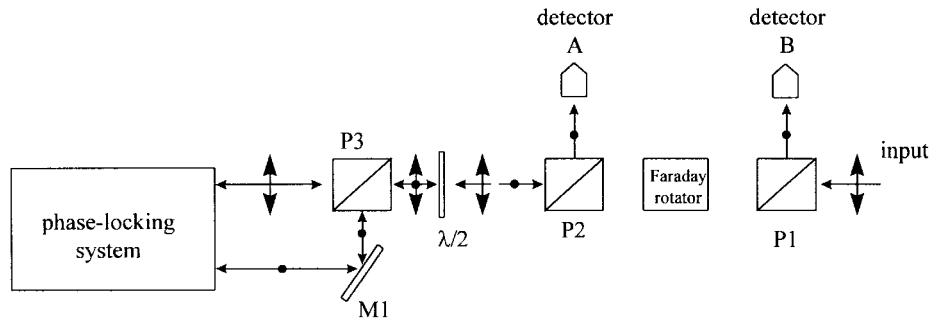


Fig. 3. Configuration for measuring degree of phase locking. P1 is the input polarizer to ensure vertically polarized light. P3 is the polarizer used to create to distinct polarizations for the phase-locking system. P2 is the analyzer used to separate the two possible return polarizations.

the largest angle one might encounter in the laboratory, this is still a valid approximation. Since, according to this model, the value of  $\phi_4$  does not change outside the Brillouin cell we have a fairly accurate estimate for the phases of  $\mathbf{A}_{4x}$  and  $\mathbf{A}_{4y}$  at the point where they are recombined.

The change in the phase difference of the  $x$  and  $y$  polarizations between the probe and its conjugate is thus given by

$$\begin{aligned} \Delta\phi_{xy} &\equiv (\phi_{3x} - \phi_{3y}) + (\phi_{4x} - \phi_{4y}) \\ &= \frac{\Omega\Delta L}{c} + \Delta\beta \end{aligned} \quad (6a)$$

$$\Delta\beta \cong (\phi_{1x} - \phi_{1y}) + (\phi_{2x} - \phi_{2y}). \quad (6b)$$

It is possible to adjust the phase difference  $\Delta\phi_{xy}$  by adjusting any of the parameters  $\Omega$ ,  $\Delta L$ , or  $\Delta\beta$ . All three of these parameters can be adjusted independently under a variety of experimental conditions.

The efficiencies for beam combining and optical path selection are determined by the value of  $\Delta\phi$ . For beam combining and optical path selection the efficiency has been previously calculated to be [7]

$$\eta = \frac{1}{2} \left[ 1 + \frac{2\sqrt{I_x I_y}}{I_x + I_y} \cos(\Delta\phi_{xy} - \psi) \right] \quad (7)$$

where  $\psi$  has been introduced as the phase difference at which the process is maximized. For example, beam combining without output path selection is optimized at  $\psi = 0$ , while it is optimized at  $\psi = \pi$  with output path selection.

### III. EXPERIMENTAL STUDY OF BEFWM

In our studies of BEFWM we found some results that held true regardless of the particular geometry that we used. These general properties of BEFWM will be described first, followed by some work pertaining to specific geometries.

The phase of the probe conjugate can be controlled accurately as long as it is controlled by the pump beams and does not build up from noise as in SBS. We derive the condition for phase locking using arguments similar to those used by Ridley and Scott [6]. We require that the second term on the right-hand side of (3d) dominates the initial formation of  $\mathbf{A}_4$ . Thus we have the condition that

$$|\mathbf{A}_1(\mathbf{A}_2 \cdot \mathbf{A}_3^*)\gamma| > |(\mathbf{A}_3^* \cdot \mathbf{A}_4)\mathbf{A}_3|. \quad (8)$$

We know that for the SBS process the initial noise intensity of  $I_4$  is given by the order of magnitude estimate of  $I_3 \exp(-25)$ . Taking the square of both sides of (8) and making the above substitution for  $I_4$  results in the condition for phase locking to be

$$I_1 I_2 |\gamma|^2 > I_3^2 \exp(-25) \quad (9)$$

which includes the angular dependence of the Brillouin process. The geometry shown in Fig. 3 was used to measure how well the two orthogonally polarized probe beams were phase locked to each other. The geometry is arranged such that the recombined probe beam will couple out to detector A if the two probe conjugate beams are phase locked, and it will be coupled out to detector B if they are not phase locked. If the probe conjugate pulses were both phase locked to the pump beam then they would add together to give a known total polarization state over the entire spatial profile of the beam. We considered an individual pulse to be phase locked if less than 2% of the combined energy was in the wrong polarization state, detected by detector B. There was no possibility for the two probe beams to mutually self-phase-lock to each other without the presence of the pump since they were orthogonally polarized with respect to each other. Fig. 4 displays the region in the pump/probe intensity space where the probe beam were phase locked. We believe that this is the first experimental measurement of the threshold for phase locking in a BEFWM geometry that has the wavelengths defined as in Fig. 1. In our experiment, we varied the pump and probe energies in the interaction region. We then measured the number of probe conjugate pulses that were phase locked and compared that to the total number of pulses used. A data point for Fig. 4 was considered to be in the phase-locked region of the graph if more than 95% of the pulses were phase locked according to the definition given above. Note that in the theory we assumed the minimum possible pump power for phase locking, thus only a few percent of the pulses would actually be phase locked. Since it would be difficult to measure this experimentally we chose to use the more stringent definition where 95% of the pulses were phase locked. Presumably because our experimental definition of phase locking was more stringent than that used in the theory, the slope was  $\exp(-20.5)$  which requires a stronger pump than is suggested by (9).

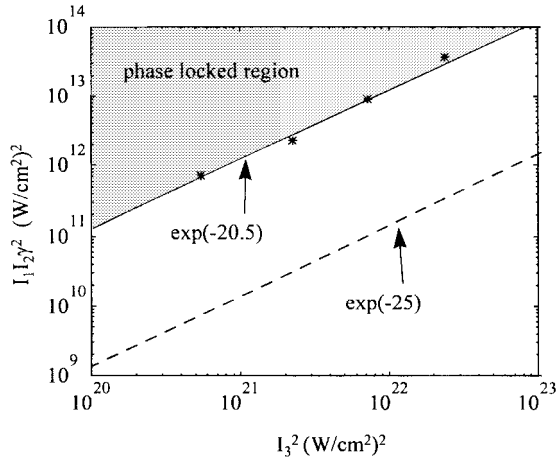


Fig. 4. The square of the probe intensity  $I_3^2$  where we started losing phase control is plotted with respect to the pump factor  $I_1 I_2 y^2$ . The solid line has a slope of  $\exp(-20.5)$  and the dashed line has a slope of  $\exp(-25)$ . The asterisks represent the maximum probe intensity for at least 95% of laser pulses having the correct output phase. This experiment was performed in Freon 113 using 10-ns pulses at 1064 nm and an angle of 35 mrad between the pump and the probe.

As can be seen from (3), there are both  $x$  and  $y$  polarization components present in a probe conjugate even when there is only one of those polarizations present in the input probe beam. Normally this orthogonal polarization component will not have a significant reflectivity since most of the gain for the  $\mathbf{A}_4$  beam is from the pure SBS gain term proportional to  $(\mathbf{A}_3^* \cdot \mathbf{A}_4)\mathbf{A}_3$  in (3d). This term will be zero for the polarization component orthogonal to  $\mathbf{A}_3$  when  $\mathbf{A}_3$  is linearly polarized. However, in some cases when splitting the polarization components of  $\mathbf{A}_3$ , it is possible to have some leakage of the orthogonal polarization through the polarizer, and thus have this term become nonzero. We found that if we had more than a few percent leakage through the polarizer we had a significant depolarization, defined as the energy in the undesired polarization divided by the total energy, in our output beam when a strongly depolarized element was placed in the probe beam line. When we had less than 2% leakage, our depolarization level was less than 2% of the total output energy. Since this is well within the specifications of the thin film polarizers that we were using we found them acceptable to use and still maintain less than 2% depolarization in our system [8].

Our studies of beam combining were carried out by splitting and recombining a single probe beam. The probe beams were separately amplified, phase conjugated, and then recombined. This can be achieved via beamsplitters or pickoffs as described above. Proper phase relationships ensured proper beam combination. Whenever the probe conjugates return to the separation points with  $\Delta\phi_{xy} = 0$  they will recombine into one beam and return back toward their origin (oscillator). They may then be directed out of the system with a Faraday rotator or a Pockels cell.

Optical path selection is one case where it may be advantageous to have  $\Delta\phi \neq 0$ . A simple 50/50 nonpolarizing beamsplitter can be used for optical path selection (Fig. 5) if it is possible to control the value of the optical phase difference,  $\Delta\phi$ . In this case the input beam would be split

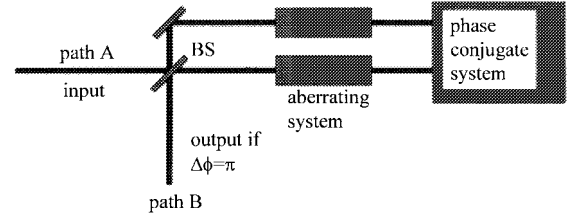


Fig. 5. A nonpolarizing beamsplitter is used to perform optical path selection. A phase difference of  $\Delta\phi = 0$  will return the beam back toward the input A, while a phase difference of  $\Delta\phi = \pi$  will send the beam out of the system along path B.

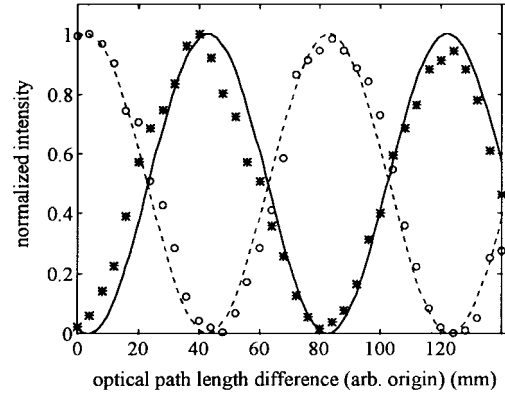


Fig. 6. The normalized output intensity is plotted as a function of the optical path length difference between the two polarization components. The asterisks and circles are experimental data incorporating a pump of circular and linear polarization, respectively. The solid and dashed lines represent the theory for circular and linear polarizations, respectively. The Brillouin active media was  $\text{CS}_2$  and the interaction length was 10 cm. This experiment was performed at low probe intensity.

via the beamsplitter. After the beamsplitter each of the new probe beams would be conjugated and phase locked. If upon recombination at the beamsplitter  $\Delta\phi = 0$  then all of the conjugate energy would return backward along its original path A and none of the light would be coupled out toward path B. If, on the other hand,  $\Delta\phi = \pi$  then all of the conjugate energy would be coupled out of the system toward path B. Thus it is possible to vary the relative phase by either changing the optical path difference or by changing the polarization ellipticity of the pump beam polarization. Fig. 6 displays the output coupling as a function of  $\Delta L$  for two values of  $\Delta\beta$ . This is different than [8, Fig. 5] where the optical path length difference was used exclusively to change the relative phase. The values for  $\Delta\beta$  were obtained using a  $\lambda/2$  plate in the pump beam for  $\Delta\beta = 2\pi$  and a  $\lambda/4$  plate for  $\Delta\beta = \pi$ . Since the optimum value of  $\psi$  in (7) is  $\pi$  to couple the beam out of the system, the optimum value of  $\Delta L$  will be  $\pi$  out of phase between the two plots. Note, for  $\text{CS}_2$ ,  $\Omega/2\pi = 3.8$  GHz which implies  $\Delta\phi_{xy} = 2\pi + \Delta\beta$  when  $\Delta L = 7.89$  cm which agrees well with our data. The slight variance of the experimental data from the theory is thought to be due to thermal heating of the  $\text{CS}_2$ , thus changing  $\Omega$  and  $\Delta L$ .

Note that it is possible to have any combination of vector phase conjugation, beam combination and optical path selection. In Section IV we describe several geometries that incorporate multiple beams, vector phase conjugation, and optical path selection.

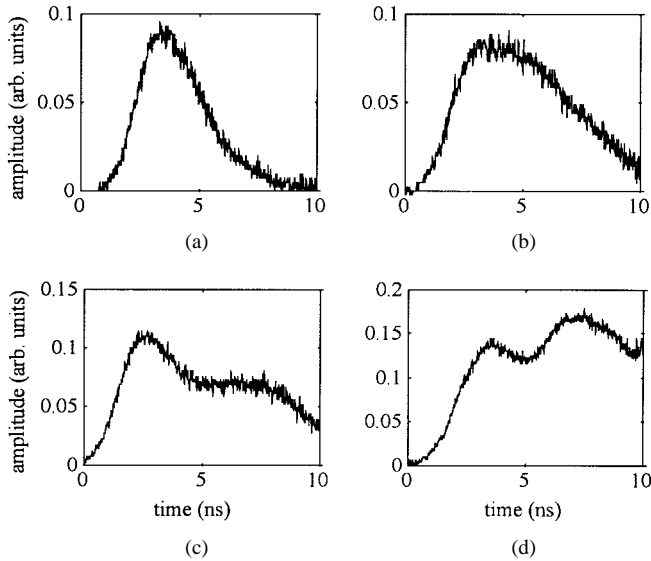


Fig. 7. The output of the system,  $|\mathbf{A}_{4x} + \mathbf{A}_{4y}|^2$ , for the cases of (a)  $\Delta\phi_{xy} = 0$ , (b)  $\Delta\phi_{xy} = 2\pi$ , (c)  $\Delta\phi_{xy} = 4\pi$ , and (d)  $\Delta\phi_{xy} = 6\pi$ . These correspond to the cases of  $\Delta L = 0, 17, 34$ , and  $51$  cm, respectively. Note that the temporal profile of the probe conjugate after recombination clearly shows that the two probe conjugates maintain the same phase relationship during the entire pulse duration when the optical path length difference is  $17$  cm or less and the Brillouin active media is Freon 113.

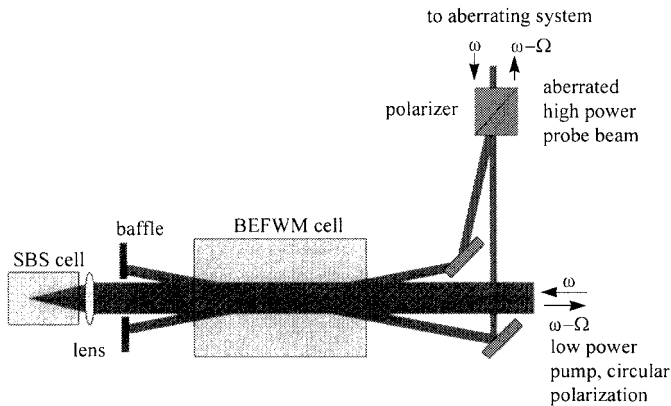


Fig. 8. Geometry that utilizes two cells containing the same Brillouin active media. The pump beam is focused into the second cell, while none of the beams, the pump or the two probes, are focused into the BEFWM cell.

It has been shown [29]–[32] that conventional SBS has random phase fluctuations in the conjugate beam every five to six times the phonon lifetime. Since, in our geometries, there is only one pump beam and it has both  $x$  and  $y$  polarization components, the conjugate of the pump beam will also have both the  $x$  and the  $y$  polarizations. Thus both the  $x$  and the  $y$  polarizations of the pump beam conjugate will experience the same phase fluctuations. The  $x$  polarized probe will interact with the  $x$  polarization in the pump and the  $y$  polarized probe will interact with the  $y$  polarization in the pump. As long as (9) is met, the phases of both probe conjugates will follow the same fluctuations as those of the single pump conjugate. During the interaction, each of the probe beams will create a conjugate in both  $x$  and  $y$  polarizations as per (3). Since the probe beam polarizations are spatially separated the orthogonal polarization of each will not lead to crosstalk and will also

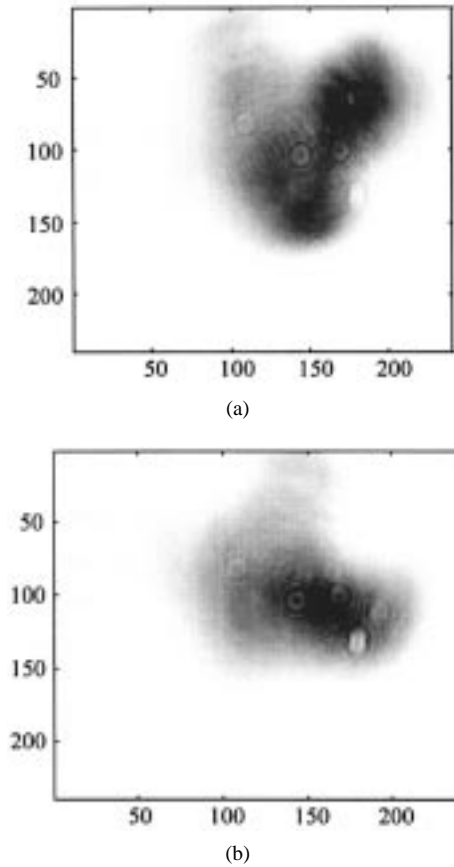


Fig. 9. Images of the near field of the (a)  $x$ -polarized and (b)  $y$ -polarized probe beams as they enter the BEFWM cell.

not experience gain from the dominant term  $(\mathbf{A}_3^* \cdot \mathbf{A}_4)\mathbf{A}_3$  in (3d). If the optical path length difference (divided by  $c/n$ ) is kept short compared to the time of phase fluctuations, then  $\Delta\phi_{xy}$  will have a negligible change during this transition period. Fig. 7 shows that for even an optical path length difference of  $17$  cm with Freon 113 as the Brillouin active media, pulse lengths of  $10$  ns, and the pump arriving at the Brillouin cell  $7$  ns before the probe, there are no significant phase fluctuations. When the optical path length difference is larger than  $17$  cm the phase fluctuations become significant. Note that, for Freon 113,  $\Delta\phi_{xy}$  is changed by  $2\pi$  in this  $17$ -cm distance which is approximately the distance the pulse would travel during the phonon lifetime, or  $1/5$  the characteristic time of the phase fluctuations. The phase of the pump conjugate, and therefore the probe conjugate, cannot change faster than the phonon lifetime [32]. Thus, the maximum optical path difference would be  $L < c\tau/n$ , where  $\tau$  is the phonon lifetime, in good agreement with our experiment. Since Freon 113 has one of the shortest phonon lifetimes ( $0.8$  ns) and smallest frequency shifts ( $\Omega/2\pi = 1.74$  GHz) for  $1\text{-}\mu\text{m}$  radiation, it can be considered a worst-case situation.

#### IV. EXPERIMENTAL GEOMETRIES FOR BEFWM

We investigated three geometries that achieve BEFWM phase conjugation with good phase control. Each of the three geometries deals with phase locking the probe beams with each other and is not intended to phase lock any probe beam

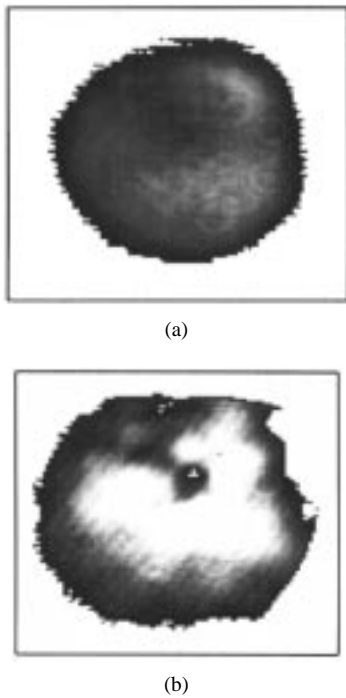


Fig. 10. Near-field images of the probe beam conjugate,  $|A_{4x} + A_{4y}|^2$ , after recombination. (a) The probe beam has very low energy (1 mJ), and thus most of the reflectivity is due to the four-wave mixing process and will be dominated by the pump beams. (b) The probe beam has 30 mJ of energy so that  $A_3$  now dominates the reflectivity. The reflectivity in (b) is 10% compared to 1% in (a). The low probe intensity image (a) has a mean of 53 counts and a standard deviation of 8. The high probe intensity image (b) has a mean of 123 counts and a standard deviation of 44 counts.

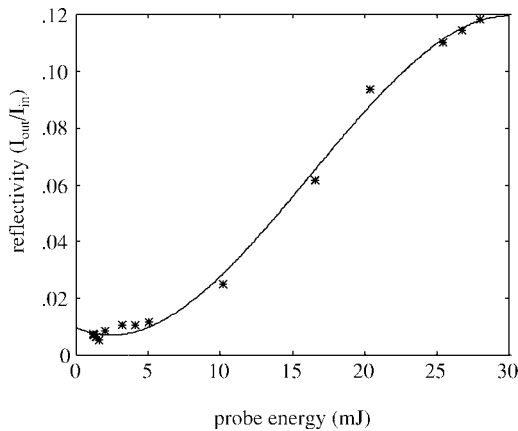


Fig. 11. Probe reflectivity for the geometry of Fig. 8. The angle between the pump and the probe was  $6^\circ$  and the probe diameter was 4 mm. The pump beam was circularly polarized and had 120 mJ of energy in a diameter of 11 mm. The line is from the theory. See text for explanation for the rise in reflectivity for low probe energies.

to the pump. The pump is not necessarily phase locked to the probe beams since it may have phase fluctuations that will not coincide temporally with the phase jumps of the probe beams. The phase jumps of the pump and probe beams can easily be achieved by incorporating a phase-locked loop [6], [7] to the SBS excitation of the pump conjugate if it were to be necessary to phase lock the pump to the probe beams.

The Nd:YAG oscillator used an optically seeded variable reflectivity unstable resonator to generate temporally

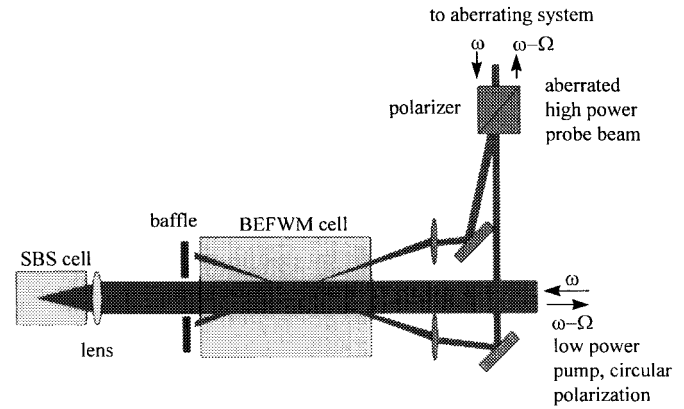


Fig. 12. The two-cell focused geometry has the pump beam focused into the second SBS cell and unfocused in the BEFWM cell. The probe beams are focused into the BEFWM cell to achieve high intensity and thus uniform high reflectivity across the entire probe beam profile.

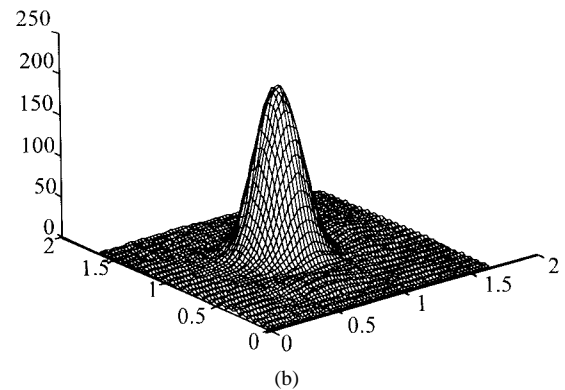
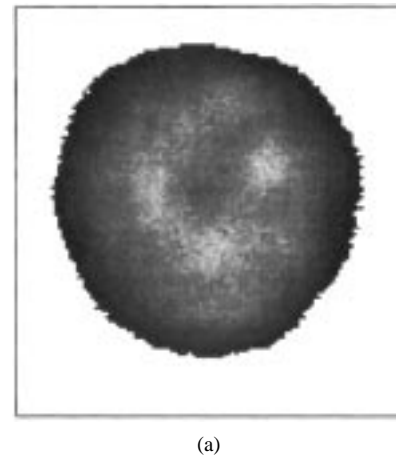


Fig. 13. (a) Near-field and (b) far-field images of the probe conjugate obtained using the geometry of Fig. 12 after recombination at the polarizer and the second pass through the aberrating system. The reflectivity was 75% for a total probe energy of 200 mJ and a pump energy of 100 mJ. The mean in (a) is 116 counts and the standard deviation is 24 counts. The beam diameter in (b) is 1.5 times larger than the diffraction-limited spot size.

transform-limited 10-ns pulses of 300 mJ of energy. The pulses from the oscillator were split into two paths, the pump and the probe. The pump had up to 120 mJ of energy with 86% of the a far-field power in a diameter of  $500 \mu\text{m}$ , which is more than ten times larger than a diffraction-limited Gaussian pulse. The probe was spatially filtered and attenuated to less than 5 mJ of

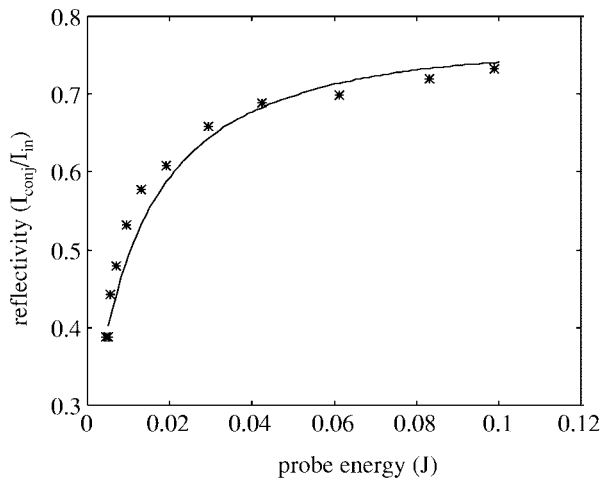


Fig. 14. Reflectivity is plotted versus the probe beam energy for a constant pump energy of 120 mJ of energy for the geometry of Fig. 12. The focused geometry increases the average intensity and thus the reflectivity is much higher than in the unfocused geometry.

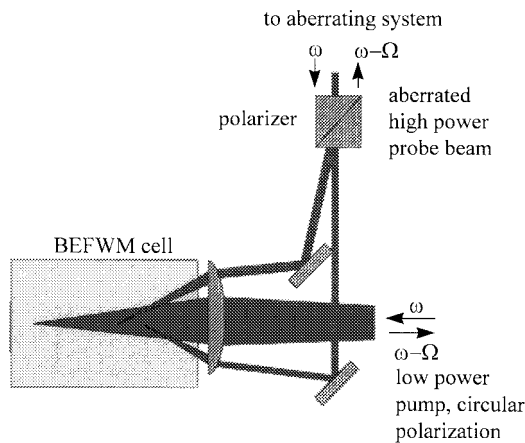


Fig. 15. The single-cell geometry is very compact, but still maintains all the advantages of the two-cell geometry shown in Fig. 12.

energy in a pulse with 86% of its far-field power in a diameter of  $75 \mu\text{m}$ , two times larger than a diffraction-limited pulse with a super-Gaussian spatial profile. An amplifier was used to increase the probe energy for the experiments. This resulted in stress-induced birefringence and wavefront aberrations on each of the probe beams. The Brillouin cell contained room-temperature Freon 113 cycled once per week through a  $1\text{-}\mu\text{m}$  filter.

#### A. Two-Cell Unfocused BEFWM

In this geometry, none of the pump or probe beams is focused into the BEFWM cell. The pump beam is conjugated using conventional SBS in a second cell placed near the BEFWM cell (Fig. 8). Each beam was assumed to be collimated in the interaction region of the BEFWM cell. The probe beam was 4 mm in diameter and the pump beam was 15 mm in diameter in the BEFWM interaction region. The pump pulses contained 120 mJ of energy and were circularly polarized.

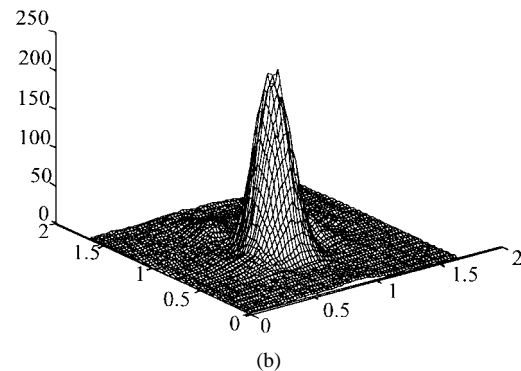
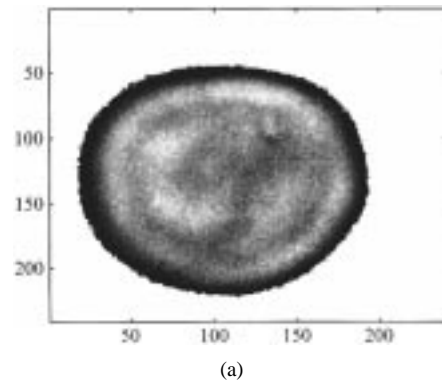


Fig. 16. The beam quality was good for the geometry of Fig. 12 as can be seen in (a) the near-field image with a mean of 108 counts and a standard deviation of 19 counts and (b) the far-field with a diameter that was 1.5 times larger than the diffraction-limited spot size. The reflectivity was 75% for a total probe energy of 200 mJ and a pump energy of 100 mJ.

The probe beams were linearly polarized orthogonal to each other and their energy and angle with respect to the pump were varied. This prevented cross coupling between the probe beams and ensured that each probe was phase locked only to the pump and its conjugate. The BEFWM cell was 445 mm long and was 80 mm from the SBS cell where the pump beam was conjugated using a lens with a focal length of 15 cm. Thus the pump conjugate was delayed by 2.8 ns with respect to the pump pulse. The pump beam  $A_1$  preceded the probe beams  $A_{3x}$  and  $A_{3y}$  by 7 ns. We chose this timing as it gave the highest reflectivity at lower energies implying a maximal temporal overlap of all beams inside the BEFWM cell.

Because of the unfocused geometry and the severity of the aberrations on the probe beam entering the BEFWM cell (Fig. 9), the reflectivity was not uniform for all spatial areas of the beams at moderate probe energies. This can be seen by noting that at low energies the first and second term of the right-hand side (RHS) of (3d) will dominate the reflectivity, but at more moderate energies the third term on the RHS of (3d) will dominate. Thus the beam quality will be significantly better at low energies than at higher energies (Fig. 10). In addition to the aberrations on the probe beam the reflectivity is low, as shown in Fig. 11. The solid line drawn in this figure is from the theoretical prediction. The increase in reflectivity at low probe energies is real. It is due to the fact that at low probe energies the grating formed by the interference of the probe and the pump conjugate but at high probe energies

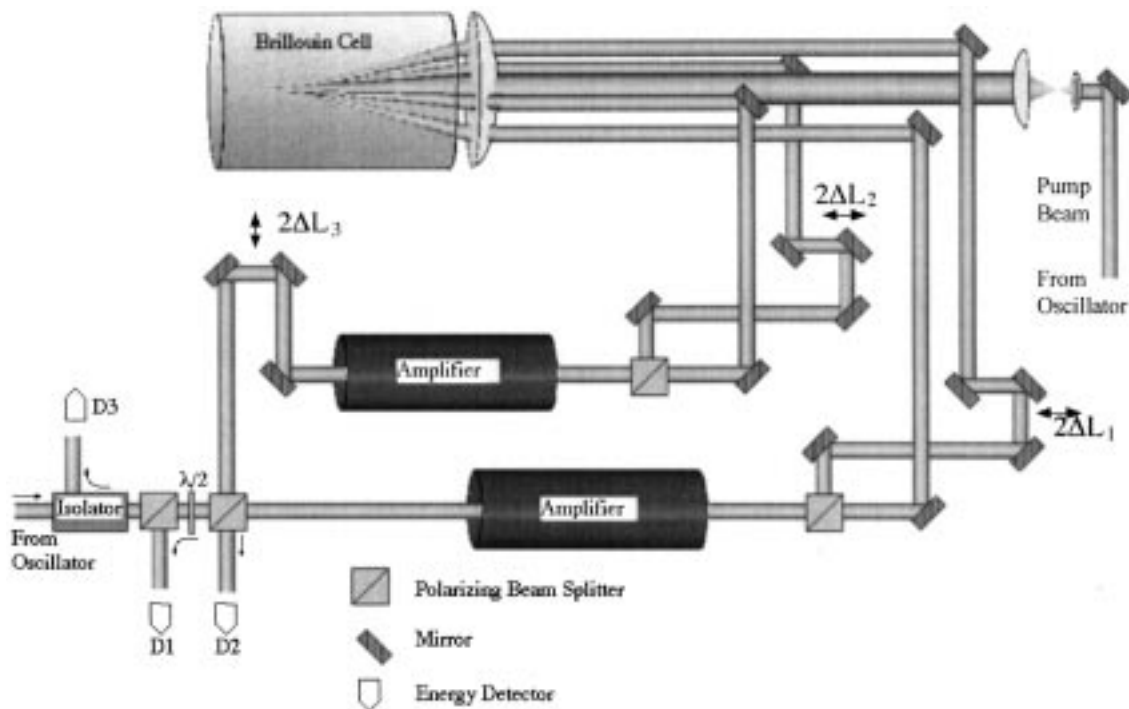


Fig. 17. Laser system that incorporates vector phase conjugation, beam combination, and optical path selection all in one geometry. Both probe beams double pass separate 25-mm amplifiers. One probe beam has an additional 12-mm amplifier and the other has an additional 9-mm amplifier, neither of which is shown for clarity. In the figure, detector D1 is used to detect the main output of the system, the depolarized light is detected at detector D2, and the residual energy after recombination and outcoupling is detected at detector D3.

the reflectivity is due mainly to the grating formed by the interference of the probe and the pump conjugate. Thus at low probe energies there is a significant fraction of the pump power coupled into the probe conjugate compared to the energy in the probe itself. This geometry was originally chosen because it does not have the high intensities associated with focusing of the pump beams into the BEFWM cell, and thus had the possibility of achieving very high probe energies without damage. But because of the reduced conjugate beam quality at the higher energies it was not suitable for our high-average-power laser application. It may, however, be suitable for some applications where the probe beam intensity is much smaller than the pump beam intensities.

### B. Two-Cell Geometry

In this geometry there are two cells containing the Brillouin active medium Freon 113. The pump beam is collimated through the first cell, the BEFWM cell, and is focused into the second cell, the SBS cell, to form the pump conjugate through the normal SBS process (see Fig. 12). The pump beam was circularly polarized with a diameter of 15 mm in the BEFWM interaction region and contained 120 mJ of energy. The probe beams were focused into the BEFWM cell using a 500-mm-focal-length lens placed such that their foci would be approximately 10 cm from the output of that 40-cm-long cell. The probe beam spot sizes were estimated to be  $300 \mu\text{m}$  and thus have a Raleigh range of 14 cm. Since the probe beams were orthogonally polarized inside the BEFWM cell, the possibility of self-phase locking without the pump

beam was eliminated. The pump beam preceded the probe beams by 7 ns as this gave the maximum reflectivity at low probe energies. The time delay for the arrival of the pump conjugate was, again, approximately 2.8 ns due to the distance from the BEFWM region to the focus of the pump beam in the SBS cell. This timing provided maximum pump intensity during the leading edge of the probe pulses. The fidelity of the probe conjugate beams was very good in both the near and far fields (Fig. 13). Approximately 86% of the beam power passed through a  $750\text{-}\mu\text{m}$  aperture using a lens with an  $F^\# = 200$ , 1.5 times larger than would be expected for a diffraction-limited beam. The maximum reflectivity of the probe beams was measured to be 70% (Fig. 14). This geometry is effective in correcting for aberrations of the wavefront and the polarization.

### C. One-Cell Geometry

In the geometry shown in Fig. 15, the pump and the probe beams are both conjugated in the same cell. The pump beam has a slight divergence at the focusing lens just before the cell. The pump and both probe beams are then focused using the same lens with a 25-cm focal length. The pump focuses to a point that is 10 cm beyond the focus of the probe beams, thus delaying the pump conjugate by 800 ps. In order for the probe beams to conjugate with good fidelity and phase locking, the pump beam must have a diameter larger than the probe beams at their focus. In addition, the intensity of the pump beam at the focus of the probe beams must meet the conditions given by (9). The maximum reflectivity of the small-signal probe beam

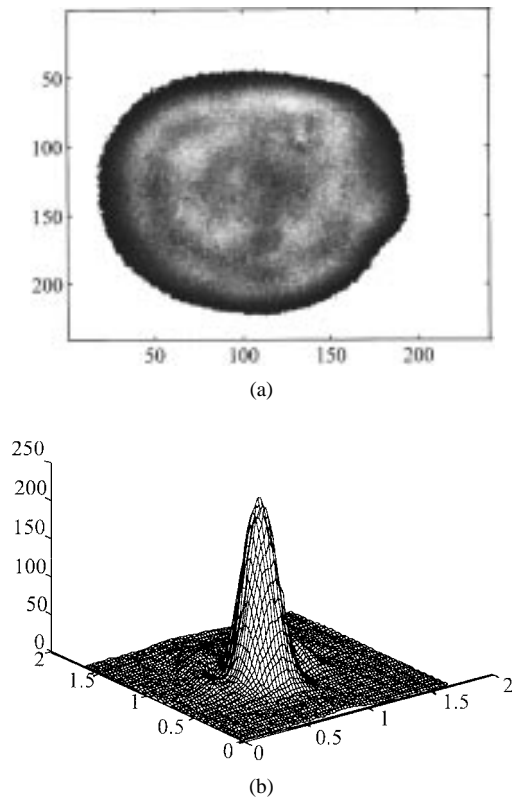


Fig. 18. (a) Near-field image of a typical 5-J pulse selected from a 10-Hz pulse train. The mean for this image is 109 counts and the standard deviation is 19 counts. (b) The far-field image is the same width as a diffraction-limited beam out to the  $1/e^2$  points. The reflectivity of the BEFWM process was 80% with a total probe energy of 500 mJ per amplifier chain and 100 mJ of pump energy.

was achieved again when the pump lead the probe by 7 ns. This is the same timing as that for the two-cell geometry. The reason for this is that the combined intensity of the pump and the probe differed by only 1 ns between the two geometries, which is at the limit of our ability to record any difference in reflectivity versus optical path length. The reflectivity of the probe beam was almost identical to that for the two-cell focused geometry shown in Fig. 15. The quality of the probe conjugate was better than 1.5 times the diffraction limit, as measured in the same manner as in the two-cell geometry, even with a highly aberrating system, as shown in Fig. 16.

## V. DESIGN OF A HIGH-POWER LASER SYSTEM

In incorporating phase conjugation into our design of a complete laser system, we chose to use the compact single-cell geometry [8]. The single-cell geometry was coupled to the laser system such that vector phase conjugation, beam combining, and optical path selection were implemented in the same system. The full system layout can be seen in Fig. 17. The oscillator is the same variable reflectivity unstable resonator used in the preceding section. We used two Nd:YAG rods that were each one inch in diameter. The single-pass gain of each rod was only four due to coupling problems between the storage capacitors and the flashlamps. When run at 10 Hz the stress-induced birefringence was very large leading

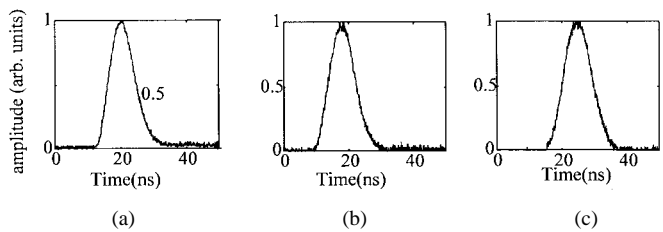


Fig. 19. Temporal traces for detectors (a) D1, (b) D2, and (c) D3 as shown in Fig. 17. Note that all traces are smooth indicating that phase fluctuations in the pump conjugate do not affect the phase relationships of the probe conjugates with respect to each other.

to about 25% of the beam in the undesired polarization in a single pass. Because of the low gain, we chose to add an additional amplifier to each arm with a single-pass gain of 20. For one arm we used a 12-mm Nd:YAG amplifier that had a large degree of single-pass birefringence ( $>25\%$ ) at 10 Hz. The other arm used a 9-mm Nd:YAG amplifier that had very little single-pass birefringence ( $<3\%$ ) at 10 Hz. The reason for the difference in the birefringence is attributed to the different physical designs of the flashlamp/rod coupling. The oscillator generated temporally transform-limited 10-ns pulses of 300 mJ of energy. The pulses for the oscillator were split into two paths, the pump and the probe. The pump had up to 120 mJ of energy in a pulse that was more than 10 times the diffraction limit in its spatial profile. The probe was spatially filtered and attenuated to less than 5 mJ of energy in a pulse of better than two times the diffraction limit. The Brillouin cell contained Freon 113 that was circulated through a  $1\text{-}\mu\text{m}$  filter once each week of operation. The lens in front of the Brillouin cell had a focal length of 25 cm. The divergence of the pump beam was such that it focused 7.3 cm behind the probe beams inside the cell. Therefore the pump was approximately 4-mm diameter at the focus of the probe beams. The probe beams had a focal spot size of approximately  $200\ \mu\text{m}$  inside the cell.

Notice that we did not need a unidirectional device to couple the energy out of the system. The Faraday isolator in the system is for monitoring the efficiency of the optical path selection and preventing any energy from returning back toward the oscillator. Detector D3 measured the residual energy that was not efficiently coupled to the output of the system toward detector D1. Detector D2 was used to measure the total depolarization from both amplifier arms. The depolarization could be measured for each amplifier individually by blocking the other arm.

Fig. 18 shows an example of a single pulse extracted from the 10-Hz pulse train at 5 J per pulse. This pulse has a diameter equal to that of a diffraction-limited pulse when measured to the  $1/e^2$  diameter, but is 1.5 times larger than the diffraction-limited spot size when measured using hard apertures that transmit 86% of the total beam energy. For maximum output out of the system, we had  $<3.8\%$  depolarization (detector D2) and  $<0.8\%$  loss from the optical path selection (detector D3). Temporal traces at maximum output for the pulses striking detectors D1–D3 can be seen in Fig. 19. Note that the traces exhibit smooth temporal profiles which implies that the phase fluctuations in the pump conjugate do not influence the phase relationships between the probe beams.

## VI. CONCLUSION

We have demonstrated that it is possible to achieve very accurate relative phase control of separately conjugated laser beams in a BEFWM phase conjugate system. We have shown that we can vary the relative phases of the conjugate beams via multiple parameters,  $\Delta k$ ,  $\Delta L$ , and  $\Delta\beta$ , the last two being the most practical for most of our applications. Our experiments demonstrate the utility of phase control for such applications as vector phase conjugation, beam combining, and optical path selection. We demonstrated the ability to have pump beams many orders of magnitude less intense than the probe beams and still lock the relative phases of the probe conjugates with respect to each other. We have also shown that optical path selection can be achieved, which eliminates the need for large unidirectional devices in certain laser systems.

We have demonstrated three geometries that can be used to control the phase of the conjugate beams, the two geometries with probe beams focused inside the BEFWM cell are applicable to our specific application, and the one-cell geometry which may be more suitable for low power applications.

We have also demonstrated that vector phase conjugation, beam combining, and optical path selection can all be achieved simultaneously for a complete laser system. We have built and tested such a laser system and shown that it can produce more than 5 J of energy with an average power of 50 W at better than 1.5 times the diffraction limit in its spatial profile.

## ACKNOWLEDGMENT

The authors wish to express their appreciation to A. Hankla and R. Stewart for their assistance with some of the experimental portions of this work. They would also like to thank K. Ridley for some helpful discussions and insights about this work.

## REFERENCES

- [1] N. G. Basov, V. F. Efimkov, I. G. Zubarev, A. V. Kotov, S. I. Mikhailov, and M. G. Smirnov, "Inversion of wavefront in SMBS of a depolarized pump," *Sov. Phys.—JETP Lett.*, vol. 28, pp. 197–201, 1978.
- [2] J. J. Ottusch and D. A. Rockwell, "Phase conjugation and polarization restoration via Brillouin-enhanced four-wave mixing," in *CLEO'91*, 1991, vol. 5, p. 50.
- [3] N. G. Basov, I. G. Zubarev, A. B. Mironov, S. I. Mikhailov, and A. Y. Okulov, "Laser interferometer with wavefront-reversing mirrors," *Sov. Phys.—JETP*, vol. 52, pp. 847–851, 1980.
- [4] N. F. Andreev, E. A. Khazanov, S. V. Kuznetsov, G. A. Pasmanik, E. I. Shklovsky, and V. S. Sidorin, "Locked phase conjugation for two-beam coupling of pulse repetition rate solid-state lasers," *IEEE J. Quantum Electron.*, vol. 27, pp. 135–141, 1991.
- [5] N. F. Andreev, E. Khazanov, and G. A. Pasmanik, "Applications of Brillouin cells to high repetition rate solid-state lasers," *IEEE J. Quantum Electron.*, vol. 28, pp. 330–341, 1992.
- [6] K. D. Ridley, "Phase-locked phase conjugation by Brillouin-induced four-wave mixing," *J. Opt. Soc. Amer. B*, vol. 12, pp. 1924–1932, 1995.
- [7] K. D. Ridley and A. M. Scott, "Phase-locked phase conjugation using a Brillouin loop scheme to eliminate phase fluctuations," *J. Opt. Soc. Amer. B*, vol. 13, pp. 900–907, 1996.
- [8] M. W. Bowers, R. W. Boyd, and A. K. Hankla, "Brillouin-enhanced four-wave-mixing vector phase conjugate mirror with beam combining capability," *Opt. Lett.*, vol. 22, pp. 360–362, 1997.
- [9] K. S. Syed, G. J. Crofts, R. P. M. Green, and M. J. Damzen, "Vectorial phase conjugation via four-wave mixing in isotropic saturable-gain media," *J. Opt. Soc. Amer. B*, vol. 14, pp. 2067–2078, 1997.
- [10] A. A. Betin, S. C. Mathews, and M. S. Mangir, "Vector phase conjugation with loop laser geometry," in *CLEO'97*, 1997, vol. 11, pp. 102–103.
- [11] N. G. Basov, V. F. Efimkov, I. G. Zubarev, A. V. Kotov, and S. I. Mikhailov, "Control of the characteristics of reversing mirrors in the amplification regime," *Sov. J. Quantum Electron.*, vol. 11, pp. 1335–1337, 1981.
- [12] D. A. Rockwell and G. R. Giuliano, "Coherent coupling of laser gain media using phase conjugation," *Opt. Lett.*, vol. 11, pp. 147–149, 1986.
- [13] M. Valley, G. Lombardi, and R. Aprahamian, "Beam combination by stimulated Brillouin scattering," *J. Opt. Soc. Amer. B*, vol. 3, pp. 1492–1497, 1986.
- [14] V. M. Leont'ev, V. G. Novoselov, Y. P. Rudnitskii, and L. V. Chernysheva, "Solid-state laser with composite active element and diffraction-limit divergence," *Sov. J. Quantum Electron.*, vol. 17, pp. 220–223, 1987.
- [15] J. Falk, M. Kanefsky, and P. Suni, "Limits to the efficiency of beam combination by stimulated Brillouin scattering," *Opt. Lett.*, vol. 13, pp. 39–41, 1988.
- [16] R. Chu, X. Hua, R. Mehringer, P. Suni, M. Kanefsky, and J. Falk, "A statistical description of stimulated Brillouin scattering beam combination efficiency," *IEEE J. Quantum Electron.*, vol. 28, pp. 1582–1593, 1992.
- [17] D. L. Carroll, R. Johnson, S. J. Pfeifer, and R. H. Moyer, "Experimental investigation of stimulated Brillouin scattering beam combination," *J. Opt. Soc. Amer. B*, vol. 9, pp. 2214–2224, 1992.
- [18] S. MacCormack and R. W. Eason, "Photorefractive techniques for diode laser beam combination," *Int. J. Nonlinear Opt. Phys.*, vol. 1, pp. 431–445, 1992.
- [19] T. R. Loree, D. E. Watkins, T. M. Johnson, N. A. Kurnit, and R. A. Fisher, "Phase locking two beams by means of seeded Brillouin scattering," *Opt. Lett.*, vol. 12, pp. 178–180, 1987.
- [20] R. H. Moyer, M. Valley, and M. C. Cimolino, "Beam combination through stimulated Brillouin scattering," *J. Opt. Soc. Amer. B*, vol. 5, pp. 2473–2489, 1988.
- [21] N. G. Basov, V. F. Efimkov, I. G. Zubarev, A. V. Kotov, S. I. Mikhailov, and M. G. Smirnov, "Inversion of wavefront in SMBS of a depolarized pump," *Sov. Phys.—JETP Lett.*, vol. 28, pp. 197–201, 1978.
- [22] K. V. Gratsianov, A. F. Kornev, V. V. Lyubimov, and V. G. Pankov, "Laser beam phasing with phase conjugation in Brillouin scattering," *Opt. Spectrosc.*, vol. 68, pp. 360–361, 1990.
- [23] I. D. Carr and D. C. Hanna, "Performance of a Nd:YAG oscillator/amplifier with phase-conjugation via stimulated Brillouin scattering," *App. Phys. B*, vol. 36, pp. 83–92, 1985.
- [24] N. F. Andreev, S. V. Kuznetsov, O. V. Palashov, G. A. Pasmanik, and E. A. Khazanov, "Four-pass YAG:Nd laser amplifier with compensation for aberration and polarization distortions of the wavefront," *Sov. J. Quantum Electron.*, vol. 22, pp. 800–802, 1992.
- [25] N. F. Andreev, O. V. Palashov, G. A. Pasmanik, and E. A. Khazanov, "Four-pass Nd:YAG laser system with compensation of aberration and polarization distortions of the wavefront," *Kvantovaya Elektronika, Moska*, vol. 23, pp. 21–24, 1996 (translated in *Quantum Electron.*, vol. 26, pp. 19–22, 1996).
- [26] V. N. Blashchuk, B. Y. Zel'dovich, V. N. Krasheninnikov, N. A. Mel'nikov, N. F. Pilipetskii, V. V. Ragul'skii, and V. V. Shkunov, "Stimulated scattering of depolarized radiation," *Sov. Phys. Dokl.*, vol. 23, pp. 588–590, 1978.
- [27] V. N. Blashchuk, V. N. Krasheninnikov, N. A. Mel'nikov, N. F. Pilipetskii, V. V. Ragul'skii, V. V. Shkunov, and B. Y. Zel'dovich, "SBS wavefront reversal for the depolarized light-theory and experiment," *Opt. Commun.*, vol. 27, pp. 137–141, 1978.
- [28] R. A. Fisher, Ed., *Optical Phase Conjugation*. Orlando, FL: Academic, 1983.
- [29] V. I. Bespalov, A. A. Betin, G. A. Pasmanik, and A. A. Shilov, "Observation of transient field oscillations in the radiation of stimulated Mandel'shtam-Brillouin scattering," *Pis'ma Zh. Eksp. Teor. Fiz.*, vol. 31, pp. 668–672, 1980; see also *JETP Lett.*, vol. 31, pp. 630–633, 1980.
- [30] N. G. Basov, I. G. Zubarev, A. B. Mironov, S. I. Mikhailov, and A. Y. Okulov, "Phase fluctuations of the Stokes wave produced as a result of stimulated scattering of light," *Pis'ma Zh. Eksp. Teor. Fiz.*, vol. 31, pp. 685–689, 1980; see also *JETP Lett.*, vol. 31, pp. 645–649, 1980.
- [31] M. V. Vasil'ev, A. L. Gyulameryan, A. V. Mamaev, V. V. Ragul'skii, P. M. Semenov, and V. G. Sidorovich, "Recording of phase fluctuations of stimulated scattered light," *Pis'ma Zh. Eksp. Teor. Fiz.*, vol. 31, pp. 673–677, 1980; see also *JETP Lett.*, vol. 31, pp. 634–638, 1980.
- [32] M. S. Mangir, J. J. Ottusch, D. C. Jones, and D. A. Rockwell, "Time-resolved measurements of stimulated-Brillouin-scattering phase jumps," *Phys. Rev. Lett.*, vol. 68, pp. 1702–1705, 1992.
- [33] R. W. Boyd, *Nonlinear Optics*. San Diego, CA: Academic, 1992, pp. 325–364.



**Mark W. Bowers** was born in Atlanta, GA, on July 8, 1964. He received the B.S. and the M.S. degrees in electrical engineering from the Georgia Institute of Technology, Atlanta, in 1986 and 1987, respectively, and the Ph.D. degree in optics from the University of Rochester, Rochester, NY, in 1997. His doctoral work involved high-power vector phase conjugation for solid-state lasers.

In 1987, he began employment at the Lawrence Livermore National Laboratory, working in the area of solid-state lasers for X-ray generation. From 1994 to 1997, he took a sabbatical to attend the University of Rochester for his doctoral studies. In 1997, he returned to Lawrence Livermore National Laboratory, Livermore, CA, where his primary research interests are in the areas of optical phase conjugation, nonlinear frequency conversion, and lidar.

**Robert W. Boyd** was born in Buffalo, NY. He received the B.S. degree in physics from the Massachusetts Institute of Technology, Cambridge, and the Ph.D. degree in physics in 1977 from the University of California at Berkeley. His Ph.D. dissertation was supervised by Charles Townes and involved the use of nonlinear optical techniques in infrared detection for astronomy.

He joined the faculty of the Institute of Optics of the University of Rochester, Rochester, NY, in 1977 and since 1987 has held the position of Professor of Optics. His research interests include studies of the nonlinear optical properties of materials, nonlinear optical interactions in atomic vapors, optical phase conjugation, and the development of new laser systems. He has advised the Ph.D. dissertations of twenty students, written two books including *Nonlinear Optics*, co-edited two anthologies, published over 160 research papers, and has been awarded four patents.

Dr. Boyd is a fellow of the Optical Society of America.